



Distribution, origin and speciation of soil selenium in the black soil region of Northeast China

Xinlin Zhong · Yiqun Gan · Yamin Deng

Received: 31 January 2020 / Accepted: 7 August 2020 / Published online: 16 August 2020
© Springer Nature B.V. 2020

Abstract Selenium (Se) is an essential trace element within human beings that hold with crucial biological functions. Investigating the complex origin of soil Se is of great importance to scientifically approach the land use of Se-rich land use, and the respective promotion of regional economic development. In this study, 160 soil samples from 10 profiles in farmland and woodland were collected in Hailun city, which is a typical black soil region in Northeast China, in order to characterize the distribution and speciation of Se in the black soil, and to identify the origin of soil Se. The total selenium content in the soil ranges from 0.045 to 0.444 $\mu\text{g g}^{-1}$, with an average selenium content in black soil (0.318 $\mu\text{g g}^{-1}$) of three times greater than that found in the yellow–brown soil (0.114 $\mu\text{g g}^{-1}$). The land-use type has a significant influence on the distribution of selenium in the black soil. Moreover, Se and heavy metals have a significant (positive or negative) correlation, in which TOC plays an important role. The black soil presents a consistent REE distribution pattern with underlying yellow–brown soil indicating black soil originates from yellow–

brown soil. REE geostatistical analysis suggests that the soil Se partly originates from shale weathering and enriches in black soil. Moreover, elemental geochemical analysis and XRD results show that the paleoclimate change from humid and warm to dry and cold is favorable for organic matter accumulation, resulting in less leaching and enhanced adsorption of selenium into the black soil.

Keywords Selenium · Black soil · Origin · Geochemistry · Sedimentary environment

Introduction

Selenium is a chalcophile nonmetallic element and was defined as an essential nutrient by the World Health Organization in the 1970s (2008; Frączek and Pasternak 2012; Statwick and Sher 2017). At proper values, selenium is beneficial for our health, for example, maintaining cells' physiological function in an ideal state, protecting cardiovascular and visual organs, maintaining myocardial health, promoting plant growth and development, and so on (Schwarz and Foltz 1999; Hatfield et al. 2014; De Temmerman et al. 2014).

Many countries and regions in the world are short of selenium; in China, more than 75% of the regions are short of selenium including Heilongjiang Province, Jilin Province, and Inner Mongolia (Dinh et al. 2018).

Electronic supplementary material The online version of this article (<https://doi.org/10.1007/s10653-020-00691-3>) contains supplementary material, which is available to authorized users.

X. Zhong · Y. Gan (✉) · Y. Deng
School of Environmental Studies, China University of Geosciences, Wuhan 430074, People's Republic of China
e-mail: yiqungan@cug.edu.cn

When humans and other organisms are deficient in selenium, they might suffer from Keshan disease (which causes necrosis of the heart muscle) and Kashin disease which causes atrophy, degeneration, and necrosis of cartilage tissue, i.e., osteochondropathy (Du et al. 2018). Conversely, excessive absorption of selenium can lead to hair loss, nail loss, and neurological disorders (Rayman 2012; Natasha et al. 2018). As is well known, selenium in plants and organisms mainly comes from soil (Xu et al. 2018). Therefore, understanding the biogeochemistry of selenium in soil is beneficial to human health and agricultural development.

Distribution of Se in soil is extremely uneven. This is directly related to soil's source. Generally speaking, the areas containing Se-rich sedimentary rock can be rich in selenium in topsoil, which has been widely observed in many areas (Wang et al. 2018, 2019; Dinh et al. 2017). According to the research of Kunli (Kunli et al. 2004) in the Daba Region of South Qinling Mountain, concentrations of selenium are different relative to the originating parent material. It was found that the overabundance of selenium is mainly related to the black lithology, in particular the black rock series of Cambrian and Sinian in China (Spadoni et al. 2007; De Temmerman et al. 2014; Hussain and Luo 2018). However, the content of selenium in soil is also related to soil characteristics, geochemistry, TOC, and Se fractions (Cheng 2003; Wen and Carignan 2007; 2008; Dhillon and Dhillon 2009).

Se in soil has four valence states: organic selenide (Se^{2-}), elemental selenium (Se^0), selenite (SeO_3^{2-}), and selenate (SeO_4^{2-}) (Kulp and Pratt 2004; Fan and Wen 2011; Favorito et al. 2017), which can be divided into five fractions according to chemical extraction method: soluble Se (SOL-Se), exchangeable and carbonate-bound Se (EX-Se), Fe–Mn oxide-bound Se (FMO-Se), organic matter-bound Se (OM-Se), and residual Se (RES-Se). Under oxidizing conditions, selenite and selenate are the major forms and highly soluble (Duc et al. 2003; Peak 2006; Hiemstra and Rietra 2007). After entering a reducing environment, both selenite and selenate will be reduced to zero-valent Se and metal selenide (Pérez-Sirvent et al. 2010; Fan and Wen 2011). Furthermore, Se can be adsorbed by iron, aluminum, and manganese hydroxides (Ma et al. 2018), where Se is usually adsorbed by internal complexation (covalent bonds or electrovalent bonds) on hydroxyl or electrostatic adsorption to

the internal or external area; this is mainly dependent on mineral or ionic strength (Duc et al. 2003). This combination can also be called FMO-Se. Besides, Luo (Luo et al. 2018) conducted a study in a selenium-rich Chongqing area, which reported that the total selenium recorded in the area was correlated with the proportion of clay components, PH, and organic matter. It was also found by Pérez-Sirvent (Pérez-Sirvent et al. 2010) that, in Spain, soil selenium measurements were related to the physical and chemical properties of soil and mineral composition; it is proportional to the percentage of quartz and has negative relationship with the percentage of calcite. In addition to these factors, organic matter is also an important factor in controlling soil selenium (Supriatin et al. 2016; Wang et al. 2017; Xie et al. 2017; Chang et al. 2019; Yin et al. 2019), which can be seen in OM-Se that represent a combination of Se and organic matter. Although the relationship between organic matter and selenium is still not very clear, it can be concluded that there are four forms (Yamada and Kamada 2009; Dinh et al. 2017; Li et al. 2017): (i) Se can be directly adsorbed to organic matter or compete the sorption sites of organic matter. (ii) Se can be part of organic matter through microbial incorporation. (iii) Se could replace S in amino acids because Se is chemically similar to S. (iv) Organic matter may directly reduce Se or be used by some microorganisms as electron donors for Se reduction.

A growing number of studies have been discussing the enrichment of selenium in soils and sediments and the occurrence and speciation of selenium in black soils. It has been found that few papers in black soil have analyzed such occurrences, and thus, they are poorly understood. Black soil, rich in organic matter, has high productivity (Kang et al. 2016). Principally for agriculture and global food production, black soil resources are crucial. In addition, the northeast of China is located in the China Se-deficient zone, and only the aforementioned black soil region has reported selenium enrichment. Therefore, the geochemical processes behind the selenium contained within black soil are of considerable research value. Some literature shows the study of selenium in black soil areas (Xia et al. 2012; Qiang et al. 2014), more specifically, the distribution of selenium and its influencing factors in the black soil of northeast China. However, these studies did not delve into the origins of Se. Moreover, little research is carried out to study the relationship

between Se and the deposition environment or the origins of Se in an area. In order to ensure the safety of local agriculture, it is necessary to compose further studies. Therefore, we choose to study the area of Hailun city, which belongs to one of the world’s three representative black soil belts. The study of soil selenium content and variation trends of Hailun city is helpful for an agricultural economy and soil resources.

The objectives of this study are (i) to characterize the distribution and speciation of Se in the black soil, (ii) to identify and clarify the origin of soil Se, and (iii) to figure out the environmental factors controlling selenium enrichment in black soils.

Methods

Study area

Hailun, located in Heilongjiang Province, Northeast China (Fig. 1), is contained in the west region of Xiaoxing’an Mountain. Its area coverage is N46°58’–47°52’ and E126°14’–127°45’, and as a reference, it can be found 214 km north of Harbin. The terrain of Hailun city belongs to a temperate continental climate, and the frost-free period is about 120 days. The topography possesses hilly qualities, with an average altitude of 239 m. In addition, Hailun’s annual precipitation is about 500–600 mm.

Soil sampling

In March 2018, 160 soil samples were collected in Hailun, consisting 10 profiles and a separate nature profile including 21 samples. The locations of these samples were recorded by GPS and are shown in Fig. 1. At each site, shovels were used to make a 50-cm-depth pit (30 × 30 cm), and then, samples were collected of the fresh topsoil. At less than a depth of 50 cm, Luoyang shovel was taken to collect samples. Samples were put in hermetic bags before their delivery to laboratory. Soil samples were air-dried, milled, and sieved with a 200 mesh.

Analytical techniques

Soil properties

Soil chemical analysis was determined by tetra-acid digestion and tested by ICP-MS. Implementing the soil suspension in ultrapure water with a 1:5 ratio, soil pH was determined. TC, TN, TS were measured via elemental analysis. TOC was determined by Vario TOC analyzer (Elemental, German) through adding 2 mol/L HCl for removing inorganic carbon and washed by ultrapure water several times.

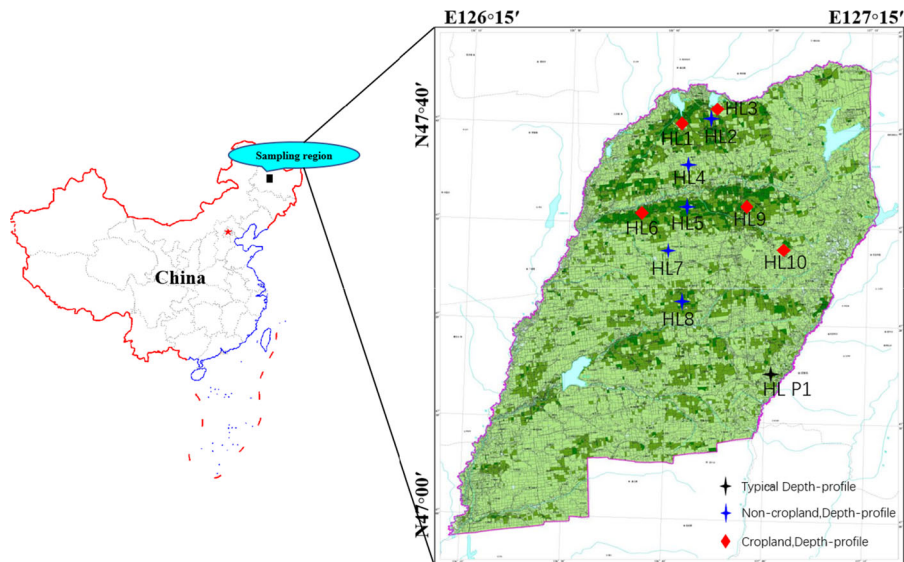


Fig. 1 Locations of study area and sampling sites. Sites were chosen farming land and woodland

Determination of Se concentration

The total Se of the soil was determined by using previous research methodology (Zhu et al. 2008). Firstly, 50 mg of soil samples was sipped in a polytetrafluoroethylene bottle; 2.5 ml 16 mol/L HNO₃ and 0.5 ml 57 mol/L HF were added into the sample bottle and heated at 150 °C for 16 h. Then, 2 ml 30% H₂O₂ was added and the bottles were heated to 90 °C, where 3 ml 6 mol/L HCl was added into the residual solution and heated to 90 °C for 2 h. The remaining solution was diluted with ultrapure water into a 50 ml PET bottle and determined by ICP-MS. The detection limit of Se by ICP-MS was 0.01 ng/g. Test quality was controlled by repeating sample testing and utilizing standard reference materials. The standard reference materials used for soil were GSS-10, GSS-11, GBW07432, GBW07410, and the accuracy of the test results is mainly controlled by inserting parallel samples and standard samples into every 10 samples. The accuracy and precision of the analyses of all samples met the required procedure specifications.

Determination of Se species

For Se speciation analysis in soil, we adopted the modified method described by Wang et al. (2012); the modified method takes into account not only Se fractionation but also the available Se species present in soil. The procedure taken is detailed as follows (Fig. S1):

- (1) Soluble Se (SOL-Se): oscillator-based extraction was performed using 0.25 M KCl at 25 °C for 1 h;
- (2) Exchangeable and carbonate-bound Se (EX-Se): 0.7 M KH₂PO₄ (pH 5.0) extract was shaken for 4 h;
- (3) Fe–Mn oxide-bound Se (FMO-Se): 2.5 M HCl was heated at 90 °C in a bath and shaken intermittently for 50 min;
- (4) Organic matter-bound Se (OM-Se): 8 mL of 5% K₂S₂O₈ and 2 mL of HNO₃ (1:1) was mixed and heated at 90 °C in a bath for 3 h. The soil–liquid ratio was 1:10 in (1) to (4).
- (5) Residual Se (RES-Se): the residue was digested with 10 mL of HNO₃ + HClO₄ (3:2) at 165 °C for 2 h.

The extract derived in (1) to (5) was used to determine Se concentration after reduction by ICP-MS.

XRD test

The clay was tested by X-ray diffractometer (XRD 7000). The XRD diffractograms were obtained at angle (3–30°), the step intervals (0.013°), the divergence slit (1/16°), the tension slit (1/8°), the receiving slit (7.5°), the voltage (40 kV), and the current (40 mA).

The rock-forming mineral was tested by X-ray diffractometer (XRD 7000). The XRD diffractograms were obtained at angle (5–90°), the step intervals (0.033°), the divergence slit (1/2°), the tension slit (1°), the receiving slit (8°), the voltage (40 kV), and the current (40 mA).

Statistical analysis

Descriptive analysis (mean, standard deviation, maximum, minimum), correlation analysis, and paired Student's *t* tests were performed using SPSS 16.0. Several correlations and profile diagrams were drawn using ORIGIN 9.0.

Result and discussion

Soil chemical characteristics

Soil pH, organic matter content, and elemental content are presented in Table 1. The TS and TN concentrations of the Hailun soil range from 0.03 to 0.33% and 0 to 0.4%, respectively, which are comparable to previous results for Hailun soils (Wang et al. 2014). No correlations were observed between TS and TSe ($p > 0.05$), but a positive relationship between TN and TSe ($p < 0.01$). TN showed a consistent decrease with depth in all cores. TOC concentrations ranged from 0.05 to 5.72% (on average 1.94%), which are comparable to previous results for Hailun soils (Wang et al. 2014; Jin et al. 2016). TOC presented a consistent decrease with depth in all cores. A positive correlation was observed between TOC and TSe ($r = 0.852$, $p < 0.01$). Selenium can be adsorbed strongly by organic matter (Supriatin et al. 2016; Dinh et al. 2017). Fe content ranged from 1.78 to 5.2%, and the average

Table 1 Basic statistical concentration of the selected elements in all samples

	TN	TOC	S	Ca	Fe	Al	pH	P	Zn	Cr	Se
Unit	%	%	%	%	%	%		μg g ⁻¹	μg g ⁻¹	μg g ⁻¹	μg g ⁻¹
Min	0.00	0.05	0.03	0.23	1.78	4.60	4.21	150	51	48	0.045
Max	0.43	5.72	0.33	3.24	5.20	8.51	8.21	1440	73	64	0.444
Average	0.11	1.94	0.11	1.03	2.93	7.37	5.31	610	61	55	0.228

Fe content is 2.93%. At 10 cores, Fe manifested a slight increase with depth and a negative correlation between Fe and TSe ($r = -0.866, p < 0.01$). Al content varied from 4.6 to 8.51% with an average of 7.37% and showed a slight increase with depth. A negative correlation was found between Al and TSe ($r = -0.859, p < 0.01$). The significant correlation between Fe, Al, TOC, and Se indicates that adsorption and competitive adsorption are present (Dinh et al. 2017) or the redox condition changes, which changes the morphology of selenium and the content of Se (Natasha et al. 2018). Ca content ranged from 0.23 to 3.24%, and the average Fe content is 1.03%. According to the 10 cores, Ca showed a slight increase with depth and a positive correlation between Ca and TSe ($r = 0.803, p < 0.01$), which might be because the leaching migration of Ca may lead to migration of Se (Zhu et al. 2015). The soil pH ranged from 4.21 to 8.21. Besides specific neutral samples, the majority of Hailun soils were acidic which may be attributed to the decaying of organic matter. Moreover, the black soil was enriched with varying degrees of heavy metals (Fig. S3.), in which Zn ($r = -0.862, p < 0.01$) and Cr ($r = -0.757, p < 0.01$) exhibited a significant negative correlation with Se. These results posed were significant differences from the characteristics of Se and heavy metals in Enshi and other places (Tao et al. 2018). It was observed that Cd possessed the same traits and presenting a significant positive correlation with Se, which is similar to the phenomenon in Enshi and other regions (Yu et al. 2014; Zhao et al. 2020). Furthermore, the TOC in Enshi and Hailun city was relatively high, which may be an important factor in controlling Cd. In this research, it was also found that heavy metals showed a significant negative correlation with TOC and a notable positive correlation with Fe, indicating that the soil-forming process had a great impact on the geochemical cycle of soil. As shown in Fig. 2 and Figure S2, HL-2 in woodland and HL-3 in farmland were selected to draw the profile element change trend diagram. The results showed that TOC,

N, Ca, and P had a decreasing trend, while Fe and Al, C value, CIA, and PIA had an increasing trend. C value shows the values of $(Fe + Al + Mn + Cr + Co + Ni)/(K + Na + Ca + Mg + Sr + Ba)$, which reflects the respective wet and dry conditions. CIA $(= Al_2O_3/(Al_2O_3 + CaO + Na_2O + K_2O))$ and PIA $(= (Al_2O_3 - K_2O)/(Al_2O_3 - K_2O + CaO + Na_2O))$ may indicate the degree of rock and soil weathering, such as CIA = 50 ~ 60 and PIA = 50–69 presenting the primary weathering intensity; CIA = 60–80 and PIA = 69–86 indicating moderate weathering intensity; and CIA = 80–100 and PIA = 86–100 denoting strong weathering intensity.

Distribution and speciation of Se in soil profiles

Total Se content is between 0.045 and 0.444 mg kg⁻¹ (on average 0.228 mg kg⁻¹) for Hailun topsoil samples (Fig. 3.). The results are within the range of previous results from Heilongjiang Province (Xia et al. 2012; Dai et al. 2015; Chi et al. 2016). Total Se content of soil above a depth of 50 cm is 0.332 mg kg⁻¹ on average. This value is higher than 0.29 mg kg⁻¹ in China and the 0.2 mg kg⁻¹ in the Songnen plain. When compared with previous studies conducted in other regions throughout the world, the average concentration of soil Se in Dashan was higher than that in Hong Kong (0.76 mg kg⁻¹), Sweden (0.30 mg kg⁻¹), and New Zealand (0.39 mg kg⁻¹). However, in Enshi and Ziyang, China, much higher soil Se proportions were found in some seleniferous areas, with amounts up to 20 mg kg⁻¹ being found (Yu et al. 2014; Long et al. 2018; Zhao et al. 2020). Essentially, the reported Se content in black soil was 0.318 mg kg⁻¹, which is 3 times higher than that found in yellow–brown soil (0.114 mg kg⁻¹).

According to the total Se concentration standards in China, five grades have been classified: deficient ($Se < 0.125$ mg kg⁻¹), marginal ($0.125 < Se < 0.175$ mg kg⁻¹), moderate ($0.175 < Se < 0.4$ mg kg⁻¹), sufficient ($0.4 < Se < 3.0$ mg kg⁻¹), and

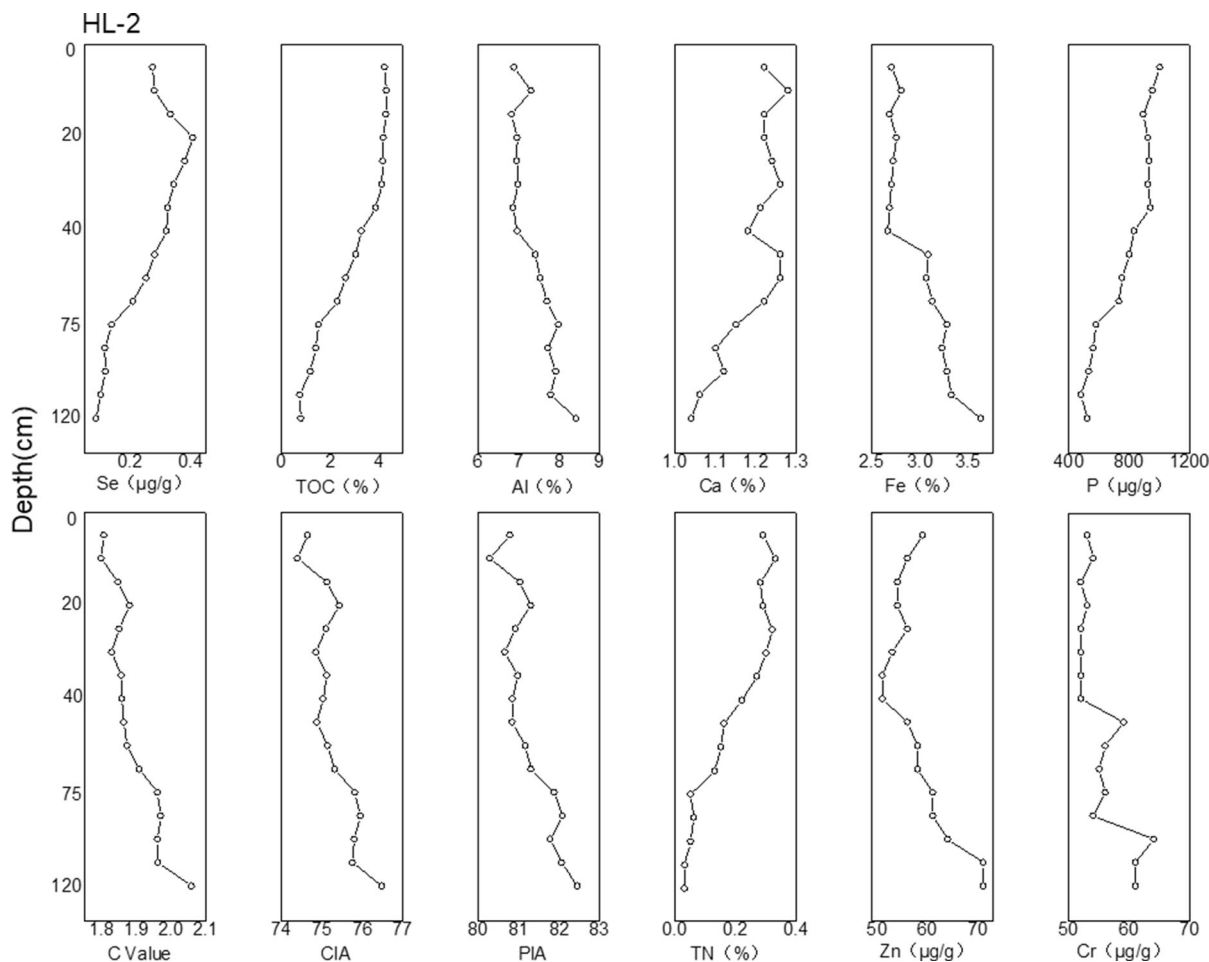


Fig. 2 Depth profiles of Se and its closely related variables in HL-2

excessive ($\text{Se} > 3.0 \text{ mg kg}^{-1}$). Therefore, Hailun city is categorized as an Se-rich area because approximately 56.02% of all samples were indexed as moderate, while 4.22% were sufficient, and additionally, about 89.66% of all samples collected above a 50 cm depth were moderate, while only 6.90% were categorized as sufficient.

According to the sampling sites (Fig. 4), the terrain of Hailun city can be divided into two types of land use: woodland and agricultural/farming land. In agricultural areas, Se concentrations are between 0.045 and 0.443 mg kg^{-1} (on average 0.227 mg kg^{-1}). In woodland, selenium concentrations are between 0.062 and 0.444 mg kg^{-1} (on average 0.231 mg kg^{-1}). In agricultural land, soil selenium changed smoothly within the 50 cm topsoil and then decreased rapidly, while in contrast, the

selenium content in the woodland areas increased slightly and then decreased. The results show that most of the Se content in black soil is moderate, while most of that found in yellow–brown soil is deficient; furthermore, the Se content in black soil is three times that in yellow–brown soil. The differences in these aforementioned zones' Se ratios may be because artificial cultivation techniques agitate surface soil so that the change of topsoil Se content is not obvious and the rapid decrease in selenium content may be due to a decreased amount of overall black soil (Yu and Zhang 2004; Aizhen et al. 2006).

Selenium speciation of the five categories of soil extraction is presented in Fig. 5. Higher than China's national average soil composition concentration of soluble selenium accounted for an average of 11.28% (with the range of 6.57% and 18.81%), which were

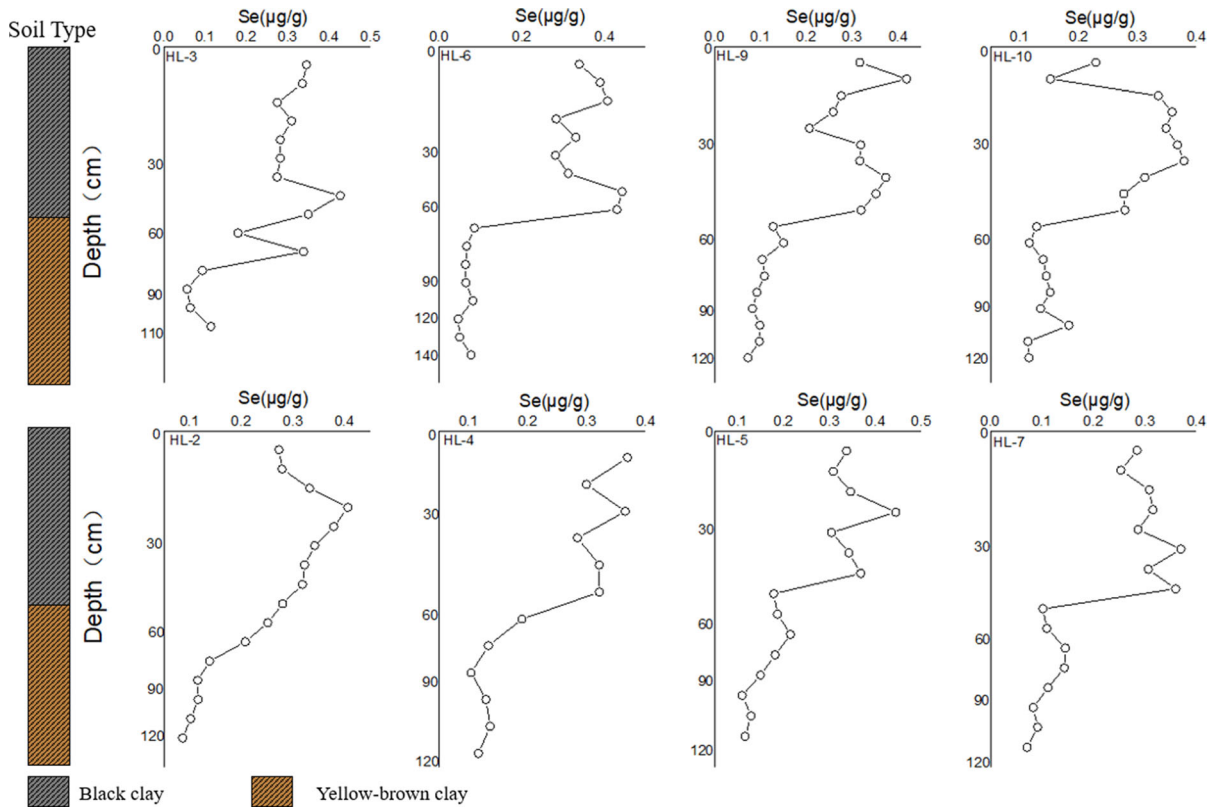


Fig. 3 Depth profiles of Se content in eight cores

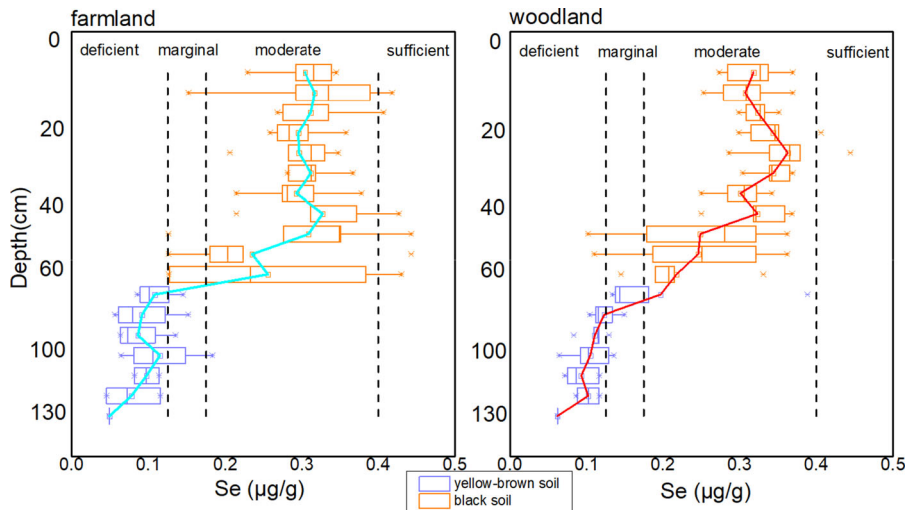


Fig. 4 Mass of Se accumulation and depth profiles of Se in farmland and woodland

11.34% in farming land and 11.16% in woodland. A significant negative correlation between SOL-Se concentration and soil S concentration ($r = -0.687$, $p < 0.05$) was observed. This relationship might be

arising on account of Se being a chalcophile element which has been shown to replace sulfur in sulfides (Pérez-Sirvent et al. 2010). Moreover, a significant positive relationship was found in concentrations of

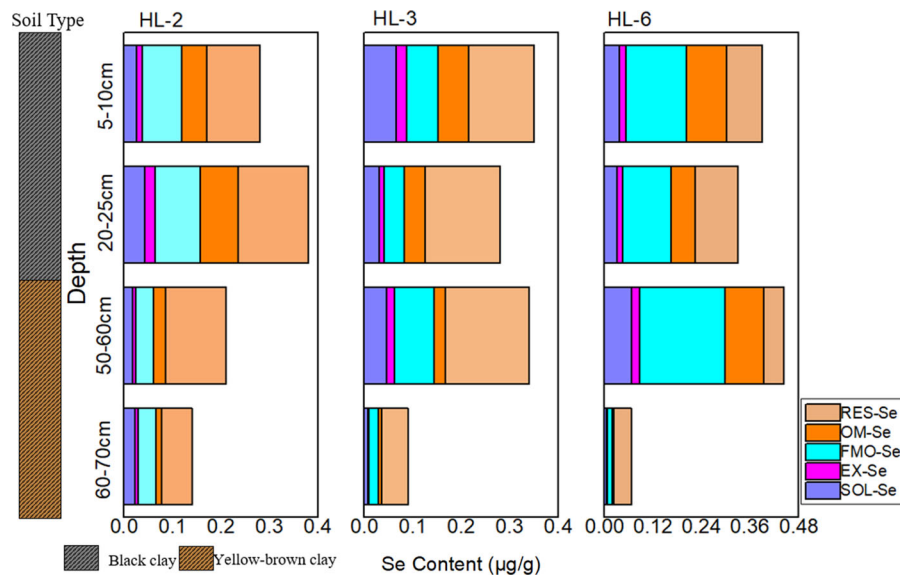


Fig. 5 Distribution of soil Se concentrations and soil Se fractions for soils collected from Hailun City, Northeast of China

SOL-Se and soil P, suggesting that soil P has some effect on SOL-Se.

Concentrations of exchangeable Se were considerably less than concentrations of soluble Se in both agricultural land and wood land, accounting for only 1.66–5.95% of total selenium. A significant positive correlation between EX-Se and soil S content, similar the relationship between SOL-Se and soil S content ($r = 0.685$, $p < 0.05$), and a significant positive correlation between EX-Se and soil S content ($r = 0.814$, $p < 0.01$) might indicate EX-Se and SOL-Se possess features allowing them to switch to each other. Conversely to SOL-Se, EX-Se concentrations had a significant positive correlation with SOM ($r = 0.624$, $p < 0.05$) and soil P ($r = 0.712$, $p < 0.01$), suggesting nutrient elements might promote the formation of EX-Se.

Concentrations of Fe/Mn oxide-bound are higher than EX-Se and SOL-Se content. Concentrations of FMO-Se accounted for an average of 26.33% (with the range between 14.98% and 47.43%), which were, separately, 27.50% in farming land and 24.00% in wood land. In particular, reaching levels of 47.43%, HL06-8 has the highest proportion of FMO-Se among all forms.

The OM-Se content was 14.83% on average, in which HL02 was relatively stable and the variation coefficient between HL03 and HL06 was notably large. The OM-Se content was recorded at 14.76% in

agricultural land on average and 14.97% in woodland on average. A significant positive correlation was observed between SOM and OM-Se concentrations ($r = 0.594$, $p < 0.05$) and also between soil N and OM-Se concentrations ($r = 0.638$, $p < 0.05$), which might indicate that the soil adsorption degree of carbon and nitrogen organic matter results in an increase in overall Se (Tolu et al. 2014; Statwick and Sher 2017).

Residual selenium accounted for the highest proportions in most selected samples, with an average of about 43.30%, accounting for 11.38%, 67.49%, respectively. The RES-Se content was 42.47% in farming land and 45.26% in woodland. A positive relationship was found between RES-Se and TSe contents ($r = 0.995$, $p < 0.01$) and between RES-Se and SOM contents ($r = 0.82$, $p < 0.05$), suggesting that SOM may play an important role in the accumulation of soil Se and RES-Se. The high content of difficult to decompose humus in the study area revealed a very strong adsorption of selenium, presenting a challenge for the decomposition of selenium in the high-selenium area as it is stored under long-term geological action (Kulp and Pratt 2004).

The origin of Se in black soils

Σ REE values of the ten profiles (Table 2) are between 145.1 and 209.2 $\mu\text{g g}^{-1}$ (on average 164.6 $\mu\text{g g}^{-1}$), which is lower than the average Chinese soil Σ REE (172.11 $\mu\text{g g}^{-1}$) and lower than that of NASC values (173.20 $\mu\text{g g}^{-1}$), indicating that the regional sedimentary Σ REE has fractionation. The $(\text{La}/\text{Yb})_n$ value, reflecting an average 10.78 the fractional distillation characteristic of LREE and HREE in the soil, which indicates the enrichment of LREE and dominance of a felsic source (Rao et al. 2018). As can be seen in Fig. 6, REE distribution curves in the section of the study area are very similar, confirming right-leaning enrichment patterns of LREE; moreover, there are obvious negative Eu anomalies.

REE is considered to be non-migratory, with only slight variations in the process of their deposition; also, source rock abundance and weathering conditions are the main factors controlling REE. Since the source material of the same soil or sediment generally has similar REE distribution patterns (Fig. 6a), the partition mode curve can be utilized to determine the characteristics of the material source. Therefore, the points dealt with chondrite values and North American shale standards were analyzed by partition mode curve analysis, and the results prove there are similar distribution curves, which are between 0 and 110 cm. With this, it can be understood that yellow–brown soil is the parent material of black soil, which is consistent with other scholars’ studies.

In addition, we compared the topsoil and underlying black shale distribution patterns of North American shale and chondrite meteorites and found that the distribution curves of the two were not parallel (Fig. 6b). Therefore, it can be considered that the parent material of black soil is not entirely derived from black shale. Since selenium has a weak correlation with rare earth elements, and black soil layers

and yellow–brown soil layers have a corresponding material source, we believe that selenium in black soil areas is greatly affected by the sedimentary environment and source of Se is not just the parent material, but other sources as well. The La/Yb–REE diagram (Fig. 6c) matches the genetic characteristics of some rocks, so as to identify the characteristics of sediment sources and provenance areas. In the figure of La/Yb– Σ REE, part of the samples in the study area fall into the calcareous mudstone area of sedimentary rocks, and also the parts falling into the granite area indicate that the material source is mainly from the mixture of calcareous mudstone and granite of sedimentary rocks. The La/V versus Th/Yb (Fig. 6d) plot shows parent material originates from a mixture of mafic and felsic sources. Thus, the weathering of mudstone and granite might be a source of soil Se (Rao et al. 2018; Kumar et al. 2019).

A collection of 21 samples, assembled according to depth for analysis purposes, was made in an exposed section of shale in the study area in order to find the source of selenium. The results showed that the Se content in the shale at the bottom was 0.911 $\mu\text{g g}^{-1}$ (Fig. S5), which was 2–4 times than that of the topsoil. Many researchers have found that the majority of the Se in the soil comes from black rocks, such as shale and mudstone. Since selenium is not entirely from the parent material, we speculate that selenium in black soil comes from black shale and acquires secondary enrichment in the black soil through weathering and transportation.

The environmental factors favorable for selenium enrichment in black soils

Principal component analysis (PCA) is a multivariate statistical analysis technique that is used to analyze the principal components of a composite system. This method is mainly used to concentrate many control

Table 2 Statistical summary of REE content collected from Hailun City, Northeast

	Σ REE	Σ LREE	Σ HREE	LREE/HREE	$(\text{La}/\text{Yb})_n$	δEu	δCe	$(\text{La}/\text{Sm})_n$	$(\text{Gd}/\text{Yb})_n$
Min	145.1	130.6	15.39	2.91	9.55	0.62	0.98	3.21	1.74
Max	209.2	191.9	21.25	3.84	14.35	0.72	1.22	4.60	2.07
Mean	164.6	148.3	17.54	3.20	10.78	0.68	1.11	3.64	1.88

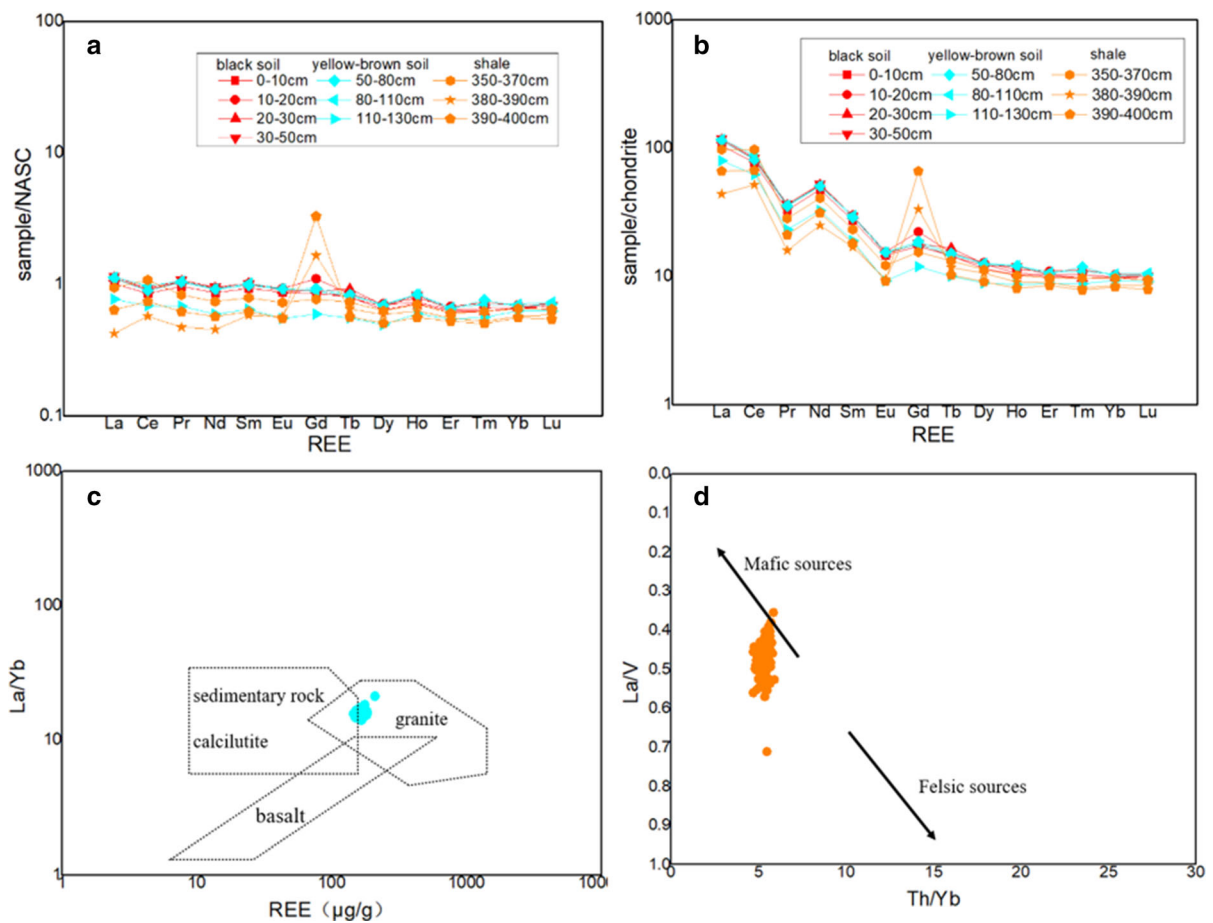


Fig. 6 **a** REE NASC distribution curve, **b** REE chondrite distribution curve, **c** La/Yb versus REE plot showing source rock feature, **d** La/V versus Th/Yb plot showing relative contributions from the felsic- and mafic-type sources in sediments

factors into a few variables; therefore, it is often used in geochemical analysis. In this study, PCA was used to identify potential influencing factors of Se. A PCA has been performed, and the results are shown in Fig. 7.

In this study, two principal components can be divided, and the first principal component is largely determined by the parent rock minerals, which are active in soil with PC1 comprised of Se, Re—Se, Li, Ti, Ca, Cr, Mg, K, Ca, Mg, and belongs to rock-forming elements (Qiang et al. 2009), furthermore Li and Ti are also a weak migration elements. The second component contains C, N, P, SOL—Se, FMO—Se, the EX—Se, and OM—Se along the PC2 vector axis. Because of the positive correlation of C, N, and P elements and depositional environment, it can be concluded that PC2 represents the sedimentary environment (climate, hydrological conditions, etc.) to a

large extent, and SOL—Se, FMO—Se, EX—Se, and OM—Se are also positively correlated with PC2.

On the other hand, PC2 is composed of elements that respond quickly to the environment and the four forms of selenium, such as C, N, P, and a combination of SOL—Se, FMO—Se, EX—Se, and OM—Se. And soil which has a positive correlation with PC2 may be an arid or semiarid region that may be subject to the freeze–thaw action, wherein the long winter, very weak soil microbial activity considerable litter, and plant residues all have difficulty quickly breaking down. After one thousand years, it can form the thick humus layer, and nutrients are easily accumulated.

According to the result of PCA, the element ratio was used to indicate the sedimentary environment indirectly. This ratio infers the environmental change by analyzing the relative migration of the corresponding elements. For example, the Fe/Mn ratio is based on

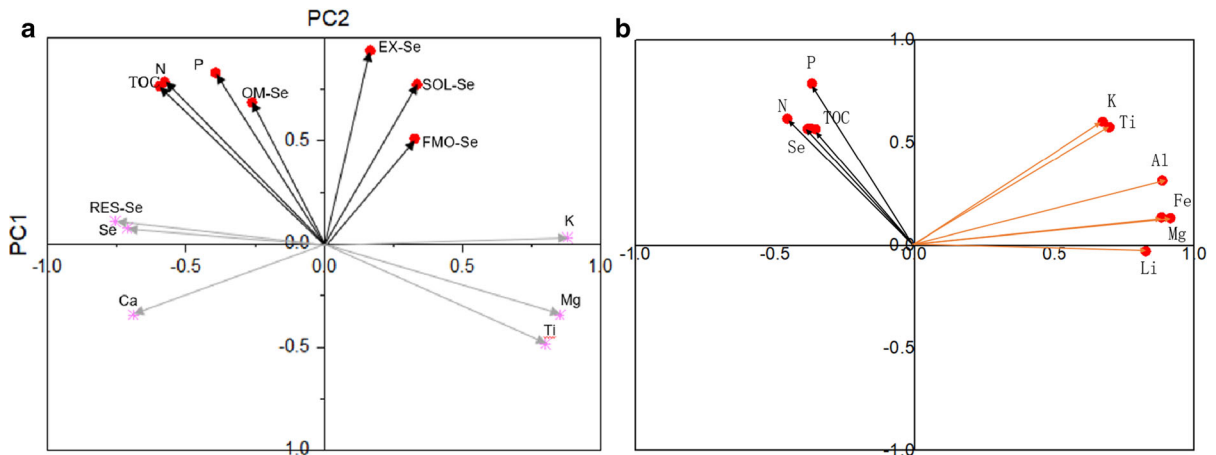


Fig. 7 PCA biplot of soil variables for elected soils collected from Hailun City, Northeast (**a** 12 points testing Se species. **b** 160 point excepting the nature profile)

the sensitivity of REDOX conditions and a higher value indicates stronger environmental reducibility; this is due to the fact that ferric iron ions are more easily oxidized than manganese ions. Ca/K values represent lower and higher temperature values. The Sr/Ca values indicate the salinity, which rises with the increase in the value. Many studies show that Rb/Sr values can elucidate the paleoclimate and a comprehensive environment C value. The results between Se and selected environmental ratios are shown in Fig. 8 and Table S1. A significant positive relationship has been observed between C and Sr/Ca ($r = 0.885, p < 0.01$) and between C and Rb/Sr ($r = 0.856, p < 0.01$). Contrarily, a significant negative

relationship has been distinguished between C and Ca/k ($r = 0.884, p < 0.01$). We can find in Fig. 8 that C values show an overall increasing trend with the increase in depth, indicating that the climate has gradually become humid and the temperature has gradually increased from top to bottom, i.e., from the present to past eras. In addition, as can be seen from the diagram, the comprehensive environment C value presented a notable negative correlation with the change of the Se ($r = 0.231, p < 0.01$), and each section has a similarly changing trend, particularly at HL05 and HL06 where the Se and integrated C change trend is very comparable, suggesting that when the climate changes into humid and higher temperatures,

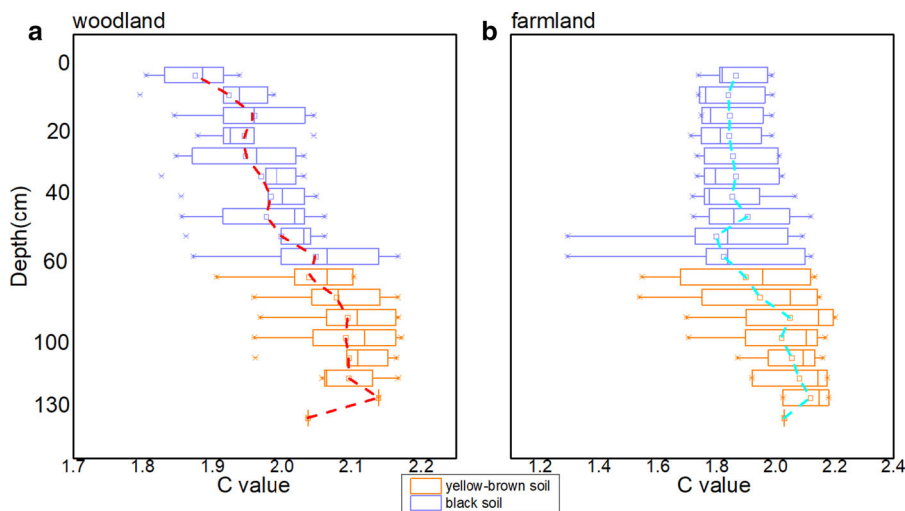


Fig. 8 Mass of environment C value accumulation and depth profiles of C value in farmland and woodland

the Se concentration steadily gets lower and vice versa; this results in an effective enrichment process. This result may be further supported by the relationship between Se and Sr/Ca.

The XRD results (Fig. 9) determined that illite content (It) at 0–40 cm was 12–69%, while illite content at 60–100 cm was 7–12%. However, the proportions of andreattite (I/S) increased considerably. It has been published that illite was formed in dry and cold climates, and when the climate gradually increased in moisture and heat, the K^+ in illite was lost, and montmorillonite was formed, which may further form kaolinite and trihydrate. An increase in I/S indicates that a climate gradually transitioned from cold to warm. Therefore, we believe that the black soil area was formed in the dry and cold climate, while yellow–brown soil areas are formed in a moist and warm climate. As can be seen above, Se mainly comes from shale weathering and is enriched in the quaternary soil. In yellow–brown soil, however, due to a damp climate, warmth, a stronger leaching effect, and lower organic matter content, Se content is decreased. Moreover, in black soil, because of low temperatures and aridity in the climate results in higher organic matter content and weaker microbial activity, thus Se

is adsorbed in organic matter and Fe/Al oxides. Consequently, Se was preserved in the black soil. The results are consistent with those shown by geochemical indicators. Therefore, we believe that the sedimentary environment can affect the migration and enrichment of Se.

Conclusion

In our work, we analyzed soil samples from Hailun city in order to understand Se distribution patterns, origin, and favorable environmental factors. In the study area, the total selenium content in the soil ranges from 0.045 to 0.444 $\mu\text{g/g}$, with an average black soil selenium content of 0.318 $\mu\text{g g}^{-1}$, which is three times higher than that found in yellow–brown soil 0.114 $\mu\text{g g}^{-1}$. The land-use type had a significant influence on the distribution of selenium in the black soil. The results show that Se content possesses a positive correlation with TOC and Fe. Most of the cases are dominated by residual selenium, followed by FMO-Se and OM-Se, including several points dominated by FMO-Se. Moreover, Se and heavy metals have a significant (positive and negative) correlation,

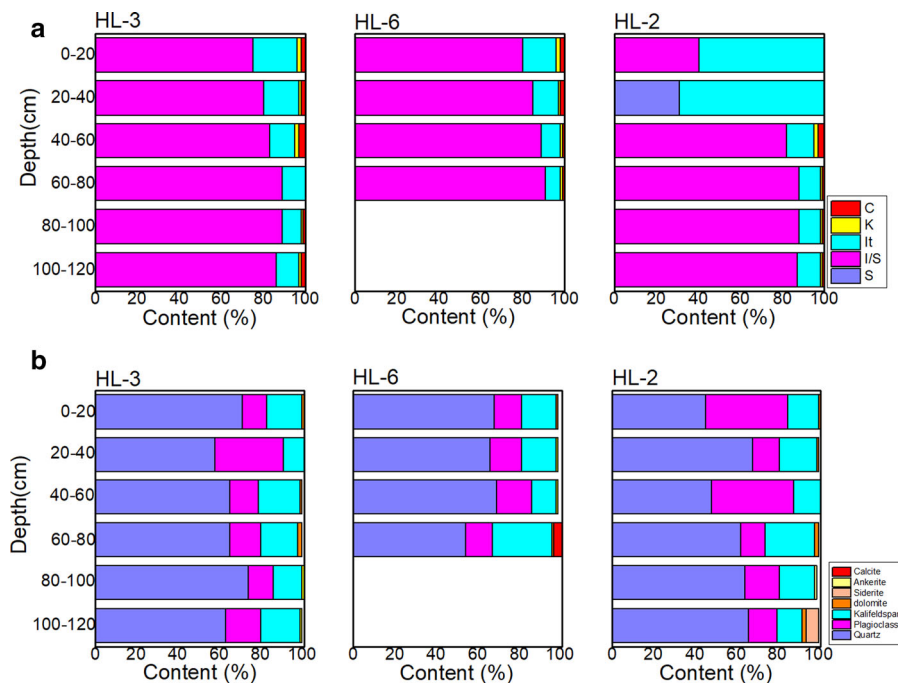


Fig. 9 Depth profiles of XRD value about petrogenetic mineral and clay mineral (a C: chlorite, K: kaolinite, It: illite, I/S: illite/montmorillonite, S: smectite)

in which TOC plays an important regulatory role. According to REE analysis, there may be two sources of selenium in black soil, with a small part of Se coming from yellow–brown soil. Moreover, the analysis results of REE indicate that part of Se may be derived from weathering shale, which was transported to Quaternary sediments, resulting in a secondary enrichment of Se. Further on this, weathering of mudstone and granite may be a source of soil Se according to REE results. It is found that the depositional environment has a certain influence on the occurrence and migration of selenium and also, the content of selenium is shown to change under different conditions. That association is also supported by PCA and XRD. Correlation analysis between selenium and some environmental indicators can also be found. For instance, under high temperature and humidity, selenium content in soil will be reduced.

This paper proves that the study area is indeed rich in selenium and emphasizes the influence of sedimentary environment on selenium distribution which has not been discussed in previous studies. In further research, ^{14}C and SEM should be added to further understand the influence of the sedimentary environment.

Acknowledgements The author was highly acknowledged to item “Investigation and evaluation of key agricultural land zones for comprehensive development and utilization in Tongliao area of Inner Mongolia” for providing laboratory facilities and financial support fieldwork.

Funding “Investigation and evaluation of key agricultural land zones for comprehensive development and utilization in Tongliao area of Inner Mongolia.”

Compliance with ethical standards

Conflicts of interest All authors declare that they have no conflict of interest.

Availability of data and material Attachment 1.

Code availability (software application or custom code) Not applicable.

References

- Aizhen, L., Xiaoping, Z., Xueming, Y., & Drury, C. F. (2006). Short-term effects of tillage on soil organic carbon storage in the plow layer of black soil in Northeast China. *Scientia Agricultura Sinica*, 39(6), 1287–1293.
- Ali-Khodja, H. (2008). Air quality and deposition of trace elements in Didouche Mourad, Algeria. *Environmental Monitoring and Assessment*, 138(1–3), 219–231. <https://doi.org/10.1007/s10661-007-9792-1>.
- Chang, C., Yin, R., Wang, X., Shao, S., Chen, C., & Zhang, H. (2019). Selenium translocation in the soil-rice system in the Enshi seleniferous area, Central China. *Science of The Total Environment*, 669, 83–90. <https://doi.org/10.1016/j.scitotenv.2019.02.451>.
- Cheng, S. (2003). Heavy metal pollution in China: origin, pattern and control. *Environmental Science and Pollution Research*, 10(3), 192–198. <https://doi.org/10.1065/espr2002.11.141.1>.
- Chi, F. Q., Kuang, E. J., Zhang, J. M., Su, Q. R., Wei, D., & Xu, Q. (2016). *Soil selenium contents, spatial distribution and their influencing factors in Heilongjiang, China (Global Advances in Selenium Research from Theory To Application)*. Boca Raton: CRC Press-Taylor & Francis Group.
- Dai, H., Gong, C., Dong, B., Liu, C., Sun, S., & Zheng, C. (2015). Distribution of soil selenium in the Northeast china plain and its influencing factors. *Acta Pedologica Sinica*, 52(6), 1356–1364.
- De Temmerman, L., Waegeneers, N., Thiry, C., Du Laing, G., Tack, F., & Ruttens, A. (2014). Selenium content of Belgian cultivated soils and its uptake by field crops and vegetables. *Science of The Total Environment*, 468–469, 77–82. <https://doi.org/10.1016/j.scitotenv.2013.08.016>.
- Dhillon, S. K., & Dhillon, K. S. (2009). Phytoremediation of selenium-contaminated soils: the efficiency of different cropping systems. *Soil Use and Management*, 25(4), 441–453. <https://doi.org/10.1111/j.1475-2743.2009.00217.x>.
- Dinh, Q. T., Cui, Z., Huang, J., Tran, T. A. T., Wang, D., Yang, W., et al. (2018). Selenium distribution in the Chinese environment and its relationship with human health: a review. *Environment International*, 112, 294–309. <https://doi.org/10.1016/j.envint.2017.12.035>.
- Dinh, Q. T., Li, Z., Tran, T. A. T., Wang, D., & Liang, D. (2017). Role of organic acids on the bioavailability of selenium in soil: a review. *Chemosphere*, 184, 618–635. <https://doi.org/10.1016/j.chemosphere.2017.06.034>.
- Du, Y., Luo, K., Ni, R., & Hussain, R. (2018). Selenium and hazardous elements distribution in plant-soil-water system and human health risk assessment of Lower Cambrian, Southern Shaanxi, China. *Environmental Geochemistry and Health* 40(5), 2049–2069. <https://doi.org/10.1007/s10653-018-0082-3>.
- Duc, M., Lefevre, G., Fedoroff, M., Jeanjean, J., Rouchaud, J. C., Monteil-Rivera, F., et al. (2003). Sorption of selenium anionic species on apatites and iron oxides from aqueous solutions. *Journal of Environmental Radioactivity*, 70(1–2), 61–72. [https://doi.org/10.1016/s0265-931x\(03\)00125-5](https://doi.org/10.1016/s0265-931x(03)00125-5).
- Fan, H., & Wen, H. (2011). Selenium speciation in Lower Cambrian Se-enriched strata in South China and its geological implications. *Geochimica et Cosmochimica Acta*, 75(23), 7725–7740. <https://doi.org/10.1016/j.gca.2011.09.027>.

- Favorito, J. E., Luxton, T. P., Eick, M. J., & Grossl, P. R. (2017). Selenium speciation in phosphate mine soils and evaluation of a sequential extraction procedure using XAFS. *Environmental Pollution*, 229, 911–921. <https://doi.org/10.1016/j.envpol.2017.07.071>.
- Frączek, A., & Pasternak, K. (2012). Selenium in medicine and treatment. *Journal of Elementology*(1/2013)., <https://doi.org/10.5601/jelem.2013.18.1.13>.
- Hatfield, D. L., Tsuji, P. A., Carlson, B. A., & Gladyshev, V. N. (2014). Selenium and selenocysteine: roles in cancer, health, and development. *Trends in Biochemical Sciences*, 39(3), 112–120. <https://doi.org/10.1016/j.tibs.2013.12.007>.
- Hiemstra, T., & Rietra, R. (2007). Surface complexation of selenite on goethite: MO/DFT geometry and charge distribution. *Croatica Chemica Acta*, 80(3–4), 313–324.
- Hussain, R., & Luo, K. (2018). Geochemical valuation and intake of F, As, and Se in coal wastes contaminated areas and their potential impacts on local inhabitants, Shaanxi China. *Environmental Geochemistry and Health*, 40(6), 2667–2683. <https://doi.org/10.1007/s10653-018-0131-y>.
- Jin, X., Du, J., Liu, H., Wang, Z., & Song, K. (2016). Remote estimation of soil organic matter content in the Sanjiang Plain, Northeast China: the optimal band algorithm versus the GRA-ANN model. *Agricultural and Forest Meteorology*, 218–219, 250–260. <https://doi.org/10.1016/j.agrformet.2015.12.062>.
- Kang, R. F., Ren, Y., Hui-Jun, W. U., & Zhang, S. X. (2016). Changes in the nutrients and fertility of black soil over 26 years in Northeast China. *Scientia Agricultura Sinica*. <http://kns.cnki.net/kcms/detail/detail.aspx?FileName=ZNYK201611008&DbName=CJFQ2016>.
- Kulp, T. R., & Pratt, L. M. (2004). Speciation and weathering of selenium in upper cretaceous chalk and shale from South Dakota and Wyoming, USA. *Geochimica et Cosmochimica Acta*, 68(18), 3687–3701. <https://doi.org/10.1016/j.gca.2004.03.008>.
- Kumar, M., Goswami, R., Awasthi, N., & Das, R. (2019). Provenance and fate of trace and rare earth elements in the sediment-aquifers systems of Majuli River Island, India. *Chemosphere*, 237, 124477. <https://doi.org/10.1016/j.chemosphere.2019.124477>.
- Kunli, L., Lirong, X., Jian'an, T., Douhu, W., & Lianhua, X. (2004). Selenium source in the selenosis area of the Daba region, South Qinling Mountain, China. *Environmental Geology*, 45(3), 426–432. <https://doi.org/10.1007/s00254-003-0893-z>.
- Li, Z., Liang, D., Peng, Q., Cui, Z., Huang, J., & Lin, Z. (2017). Interaction between selenium and soil organic matter and its impact on soil selenium bioavailability: a review. *Geoderma*, 295, 69–79. <https://doi.org/10.1016/j.geoderma.2017.02.019>.
- Long, Z., Yuan, L., Hou, Y., Banuelos, G. S., Liu, Y., Pan, L., et al. (2018). Spatial variations in soil selenium and residential dietary selenium intake in a selenium-rich county, Shitai, Anhui, China. *Journal of Trace Elements in Medicine and Biology*, 50, 111–116. <https://doi.org/10.1016/j.jtemb.2018.06.019>.
- Luo, Y., Han, G., Sun, X., Liao, D., Xie, Y., & Wei, C. (2018). Distribution of soil selenium in three Gorges Reservoir region (Chongqing Section) and its influential factors. *Soils*, 50(1), 131–138.
- Ma, B., Fernandez-Martinez, A., Grangeon, S., Tournassat, C., Findling, N., Carrero, S., et al. (2018). Selenite uptake by Ca-Al LDH: a description of intercalated anion coordination geometries. *Environmental Science & Technology*, 52(3), 1624–1632. <https://doi.org/10.1021/acs.est.7b04644>.
- Natasha, S., M., Niazi, N. K., Khalid, S., Murtaza, B., Bibi, I., et al. (2018). A critical review of selenium biogeochemical behavior in soil-plant system with an inference to human health. *Environmental Pollution*, 234, 915–934. <https://doi.org/10.1016/j.envpol.2017.12.019>.
- Peak, D. (2006). Adsorption mechanisms of selenium oxyanions at the aluminum oxide/water interface. *Journal of Colloid and Interface Science*, 303(2), 337–345. <https://doi.org/10.1016/j.jcis.2006.08.014>.
- Pérez-Sirvent, C., Martínez-Sánchez, M. J., García-Lorenzo, M. L., Molina, J., Tudela, M. L., Mantilla, W., et al. (2010). Selenium content in soils from Murcia Region (SE, Spain). *Journal of Geochemical Exploration*, 107(2), 100–109. <https://doi.org/10.1016/j.gexplo.2010.10.001>.
- Qiang, F. U., Wang, D. Y., Yue-Fen, L. I., Yang, X. L., & Yang, Y. Y. (2014). Pedogeochemical research on Se in black soil areas of central Jilin Province. *Global Geology*. <http://kns.cnki.net/kcms/detail/detail.aspx?FileName=SJDZ201401011&DbName=CJFQ2014>.
- Qiang, S. H. U., Zhi-jun, Z., Ye, C., Mao-heng, Z., & Ji-jun, L. I. (2009). Palaeoenvironmental significance of geochemistry elements and grain size of DS core sediments in Xinghua, Jiangsu Province. *Scientia Geographica Sinica*, 29(6), 923–928.
- Rao, G. W., Liu, X. D., & Liu, P. H. (2018). REE geochemical characteristics and material sources of claystone of the upper member of the banyan gobi formation in tamsag. *Acta Geologica Sichuan*. <http://kns.cnki.net/kcms/detail/detail.aspx?FileName=SCDB201801010&DbName=CJFQ2018>.
- Rayman, M. P. (2012). Selenium and human health. *The Lancet*, 379(9822), 1256–1268. [https://doi.org/10.1016/s0140-6736\(11\)61452-9](https://doi.org/10.1016/s0140-6736(11)61452-9).
- Schwarz, K., & Foltz, C. M. (1999). Selenium as an integral part of Factor 3 against dietary necrotic liver degeneration (Reprinted from Journal of the American Chemistry Society, vol 79, pg 3292, 1957). *Nutrition*, 15(3), 255–255.
- Spadoni, M., Voltaggio, M., Carcea, M., Coni, E., Raggi, A., & Cubadda, F. (2007). Bioaccessible selenium in Italian agricultural soils: Comparison of the biogeochemical approach with a regression model based on geochemical and pedoclimatic variables. *Science of the Total Environment*, 376(1–3), 160–177. <https://doi.org/10.1016/j.scitotenv.2007.01.066>.
- Statwick, J., & Sher, A. A. (2017). Selenium in soils of western Colorado. *Journal of Arid Environments*, 137, 1–6. <https://doi.org/10.1016/j.jaridenv.2016.10.006>.
- Supriatin, S., Weng, L., & Comans, R. N. J. (2016). Selenium-rich dissolved organic matter determines selenium uptake in wheat grown on Low-selenium arable land soils. *Plant and Soil*, 408(1–2), 73–94. <https://doi.org/10.1007/s11104-016-2900-7>.

- Tao, Y., Zhongfang, Y., Rui, W., Qingliang, Z., Wanling, H., & Science, S. O. (2018). Characteristics and sources of soil selenium and other elements in typical high selenium soil area of Enshi. *Soils*. <http://kns.cnki.net/kcms/detail/detail.aspx?FileName=TURA201806010&DbName=CJFQ2018>.
- Tolu, J., Thiry, Y., Bueno, M., Jolivet, C., Potin-Gautier, M., & Le Hecho, I. (2014). Distribution and speciation of ambient selenium in contrasted soils, from mineral to organic rich. *Science of the Total Environment*, 479–480, 93–101. <https://doi.org/10.1016/j.scitotenv.2014.01.079>.
- Wang, D., Dinh, Q. T., Anh Thu, T. T., Zhou, F., Yang, W., Wang, M., et al. (2018). Effect of selenium-enriched organic material amendment on selenium fraction transformation and bioavailability in soil. *Chemosphere*, 199, 417–426. <https://doi.org/10.1016/j.chemosphere.2018.02.007>.
- Wang, D., Xue, M. Y., Wang, Y. K., Zhou, D. Z., Tang, L., Cao, S. Y., et al. (2019). Effects of straw amendment on selenium aging in soils: Mechanism and influential factors. *Science of the Total Environment*, 657, 871–881. <https://doi.org/10.1016/j.scitotenv.2018.12.021>.
- Wang, D., Zhou, F., Yang, W., Peng, Q., Man, N., & Liang, D. (2017). Selenate redistribution during aging in different Chinese soils and the dominant influential factors. *Chemosphere*, 182, 284–292. <https://doi.org/10.1016/j.chemosphere.2017.05.014>.
- Wang, S., Liang, D., Wang, D., Wei, W., Fu, D., & Lin, Z. (2012). Selenium fractionation and speciation in agriculture soils and accumulation in corn (*Zea mays* L.) under field conditions in Shaanxi Province, China. *The Science of the Total Environment* 427–428, 159–164. <https://doi.org/10.1016/j.scitotenv.2012.03.091>.
- Wang, W., Wang, H., & Zu, Y. (2014). Temporal changes in SOM, N, P, K, and their stoichiometric ratios during reforestation in China and interactions with soil depths: Importance of deep-layer soil and management implications. *Forest Ecology and Management*, 325, 8–17. <https://doi.org/10.1016/j.foreco.2014.03.023>.
- Wen, H., & Carignan, J. (2007). Reviews on atmospheric selenium: Emissions, speciation and fate. *Atmospheric Environment*, 41(34), 7151–7165. <https://doi.org/10.1016/j.atmosenv.2007.07.035>.
- Xia, X., Yang, Z., Xue, Y., Cui, Y., Li, Y., Hou, Q., et al. (2012). Geochemical Circling of Soil Se on the Southern Song-Nen Plain, Heilongjiang Province. *Geoscience*, 26(5), 850.
- Xie, Y., Dong, H., Zeng, G., Zhang, L., Cheng, Y., Hou, K., et al. (2017). The comparison of Se(IV) and Se(VI) sequestration by nanoscale zero-valent iron in aqueous solutions: the roles of solution chemistry. *Journal of Hazardous Materials*, 338, 306–312. <https://doi.org/10.1016/j.jhazmat.2017.05.053>.
- Xu, Y., Li, Y., Li, H., Wang, L., Liao, X., Wang, J., et al. (2018). Effects of topography and soil properties on soil selenium distribution and bioavailability (phosphate extraction): a case study in Yongjia County, China. *Science of the Total Environment*, 633, 240–248. <https://doi.org/10.1016/j.scitotenv.2018.03.190>.
- Yamada, H., & Kamada, A. (2009). Total selenium content of agricultural soils in Japan. *Soil Science and Plant Nutrition*, 55(5), 616–622. <https://doi.org/10.1111/j.1747-0765.2009.00397.x>.
- Yin, H., Qi, Z., Li, M., Ahammed, G. J., Chu, X., & Zhou, J. (2019). Selenium forms and methods of application differentially modulate plant growth, photosynthesis, stress tolerance, selenium content and speciation in *Oryza sativa* L. *Ecotoxicology and Environmental Safety*, 169, 911–917. <https://doi.org/10.1016/j.ecoenv.2018.11.080>.
- Yu, L., & Zhang, B. (2004). The degradation situations of black soil in China and its prevention and counter measures. *Journal of Arid Land Resources and Environment*, 18(1), 99–103.
- Yu, T., Yang, Z., Lv, Y., Hou, Q., Xia, X., Feng, H., et al. (2014). The origin and geochemical cycle of soil selenium in a Se-rich area of China. *Journal of Geochemical Exploration*, 139, 97–108. <https://doi.org/10.1016/j.gexplo.2013.09.006>.
- Zhao, B., Xing, C., Zhou, S., Wu, X., Yang, R., & Yan, S. (2020). Sources, Fraction Distribution and Health Risk Assessment of Selenium (Se) in Dashan Village, a Se-Rich Area in Anhui Province. *Bulletin of Environmental Contamination and Toxicology* 104(4), 545–550. <https://doi.org/10.1007/s00128-020-02827-8>.
- Zhu, J., Wang, N., Li, S., Li, L., Su, H., & Liu, C. (2008). Distribution and transport of selenium in Yutangba, China: impact of human activities. *Science of the Total Environment*, 392(2–3), 252–261. <https://doi.org/10.1016/j.scitotenv.2007.12.019>.
- Zhu, X., Liu, X., Liu, J., Tang, Q., & Meng, T. (2015). Contents and distributions characteristic of selenium in natural soil profile samples from the Western Sichuan Plateau Area. *Ecology & Environmental Sciences*. <http://kns.cnki.net/kcms/detail/detail.aspx?FileName=TRYJ201504019&DbName=CJFQ2015>.

Publisher's Note Springer Nature remains neutral with regard to jurisdictional claims in published maps and institutional affiliations.